Journal of Pharmaceutical and Biomedical Analysis 229 (2023) 115374

Contents lists available at ScienceDirect

Journal of Pharmaceutical and Biomedical Analysis

journal homepage: www.journals.elsevier.com/journal-of-pharmaceutical-and-biomedical-analysis

In Vivo evaluation of newly synthesized ^{213}Bi-conjugated alpha-melanocyte stimulating hormone (α-MSH) peptide analogues in melanocortin-1 receptor (MC1-R) positive experimental melanoma model

Ibolya Kálmán-Szabó [a,b,1], Zita Képes [a,*,1], Anikó Fekete [a], Adrienn Vágner [c], Gábor Nagy [c], Dániel Szücs [a,d,e], Barbara Gyuricza [a,e], Viktória Arató [a,f], József Varga [a], Levente Kárpáti [g], Ildikó Garai [a,c], István Mándity [g,h], Frank Bruchertseifer [i], János Elek [j,k], Dezs Szikra [a], György Trencsényi [a,b]

[a] Division of Nuclear Medicine and Translational Imaging, Department of Medical Imaging, Faculty of Medicine, University of Debrecen, Nagyerdei St. 98, H-4032 Debrecen, Hungary
[b] Gyula Petrányi Doctoral School of Clinical Immunology and Allergology, Faculty of Medicine, University of Debrecen, Nagyerdei St. 98, H-4032 Debrecen, Hungary
[c] Scanomed Ltd., Debrecen, Nagyerdei St. 98, H-4032 Debrecen, Hungary
[d] Department of Physical Chemistry, Faculty of Science and Technology, University of Debrecen, Egyetem square 1, H-4032 Debrecen, Hungary
[e] Doctoral School of Chemistry, Faculty of Science and Technology, University of Debrecen, Egyetem square 1, H-4032 Debrecen, Hungary
[f] Doctoral School of Pharmaceutical Sciences, University of Debrecen, Nagyerdei St. 98, H-4032 Debrecen, Hungary
[g] Department of Organic Chemistry, Faculty of Pharmacy, Semmelweis University, Hőgyes Endre St. 7, H-1092 Budapest, Hungary
[h] Artificial Transporters Research Group, Research Centre for Natural Sciences, Magyar tudósok boulevard 2, H-1117 Budapest, Hungary
[i] European Commission, Joint Research Centre (JRC), Karlsruhe, Germany
[j] Department of Inorganic and Analytical Chemistry, University of Debrecen, Nagyerdei St. 98, H-4032 Debrecen, Hungary
[k] Science Port Ltd., Debrecen, Elek St. 166, H-4225 Debrecen, Hungary

ARTICLE INFO

Keywords:
Alpha-melanocyte stimulating hormone-analogue (α-MSH analogue)
[^{213}Bi]Bi-DOTA-FOLDamide
[^{213}Bi]Bi-DOTA-HOLDamide
[^{213}Bi]Bi-DOTA-MARSamide
[^{213}BiBi -DOTA-NAPamide
Melanocortin-1 receptor (MC1-R)

ABSTRACT

Given the rising pervasiveness of melanocortin-1 receptor (MC1-R) positive melanoma malignum (MM) and pertinent metastases, radiolabelled receptor-affine alpha-melanocyte stimulating hormone-analogue (α-MSH analogue) imaging probes would be of crucial importance in timely tumor diagnostic assessment. Herein we aimed at investigating the biodistribution and the MM targeting potential of newly synthesized ^{213}Bi-conjugated MC1-R specific peptide-based radioligands with the establishment of MC1-R overexpressing MM preclinical model. DOTA-conjugated NAP, -HOLD, -FOLD, -and MARSamide were labelled with ^{213}Bi. *Ex vivo* biodistribution studies were conducted post-administration of 3.81 ± 0.32 MBq [^{213}Bi]Bi-DOTA conjugated deriva-tives into twenty B16-F10 tumor-bearing C57BL/6 J and healthy mice. Organ Level Internal Dose Assessment (OLINDA) and IDAC-Dose were used to calculate translational data-based absorbed radiation dose in human organs. Moderate or low %ID/g uptake of [^{213}Bi]Bi-DOTA conjugated NAP, -HOLD, -and MARSamide and significantly increased [^{213}Bi]Bi-DOTA-FOLDamide accumulation was observed in the thoracic and abdominal organs ($p \leq 0.01$). High [^{213}Bi]Bi-DOTA-NAP (%ID/g:3.76 ± 0.96), -and FOLDamide (%ID/g:3.28 ± 0.95) tumor tracer activity confirmed their MC1-R-affinity. The bladder wall received the highest radiation absorbed dose followed by the kidneys (bladder wall: $1.95{\cdot}10^{-2}$ and $8.97{\cdot}10^{-2}$ mSv/MBq; kidneys: $7.47{\cdot}10^{-3}$ vs. $5.88{\cdot}10^{-2}$ mSv/MBq measured by IDAC and OLINDA; respectively) indicating the suitability of the NAPamide derivative for clinical use. These novel [^{213}Bi]Bi-DOTA-linked peptide probes displaying meaningful MC1-R affinity could be promising molecular probes in MM imaging.

* Corresponding author.
E-mail address: kepes.zita@med.unideb.hu (Z. Képes).
[1] These authors contributed equally to this study

https://doi.org/10.1016/j.jpba.2023.115374
Received 30 January 2023; Received in revised form 27 March 2023; Accepted 27 March 2023
Available online 28 March 2023

1. Introduction

Melanocytes-originated Malignant Melanoma (MM) - *postulated as the most aggressive skin carcinoma* - is responsible for approximately 65% of overall skin cancer-associated deaths. Immense metastatic spread to various distant localizations including the brain, the lungs, and the liver accounts for 5-year survival rates of only 5–19%. The rapidly increasing worldwide incidence of MM and subsequent cancer-related mortality have spurred clinical interest in the early diagnostic assessment as well as the proposal of novel therapeutic approaches of this malignancy and pertinent metastases [1]. Multiple non-invasive imaging techniques such as Positron Emission Tomography (PET) and Single Photon Emission Computed Tomography (SPECT) with the application of specific tumor targeted diagnostic probes and directed anti-tumor therapeutic agents may represent a breakthrough in patients' survival suffering from MM [2]. Since several MM-specific genuine radiopharmaceuticals have already been developed and synthesized in the field of isotope diagnostics, nuclear medical imaging may not fall short in providing promising radiolabelled vectors for the timely detection of both primary neoplasms and relevant metastases.

The widespread application of melanoma-associated antibodies and melanin-specific benzamide derivatives labelled with radioisotopes is regarded as a landmark in MM imaging [2]. Given that ample amount of evidence strengthens the overexpression of melanocortin-1 receptor (MC1-R) in MM tumor cells, outstanding attention has been placed upon the development of MC1-R-affine diagnostic and therapeutic radiotracers in the management of MM. MC1-R - *triggered by α-melanocyte-stimulating hormone (α-MSH)* - has pivotal role in controlling pigmentation as well as cell proliferation [2].

Further, prior research data indicated the specific MC1-R targeting capability of α-MSH analogue NAPamide (Ac-Nle-Asp-His-D-Phe-Arg-Trp-Gly-Lys-NH_2) and DOTA-NAPamide **(1)** as well [3]. In addition, the feasibility of MC1-R-related NAPamide labelled with Copper-64 (^{64}Cu), Gallium-68 (^{68}Ga), Fluorine-18 (^{18}F), Indium-111 (^{111}In), Scandium-44 (^{44}Sc) and Technetium-99 m ($^{99\ m}$Tc) was also strengthened in the detection of MM applying *in vivo* imaging techniques [2–6]. Besides diagnostic application however, MC1-R-targeted therapeutic radiotracers with α-, β- radiation or Auger electron emission, may lead to the establishment of tailor-made melanoma guidance. Currently existing MC1-R-directed ReO cyclized DOTA-[$Cys^{3,4,10}$,D-Phe^{7}]alpha-$MSH_{3–13}$ (CCMSH) probes including ^{188}Re-(Arg^{11})CCMSH, [^{212}Pb]Pb-DOTA-Re(Arg^{11})CCMSH, [^{177}Lu]Lu, - and [^{90}Y]Y-DOTA-Re(Arg^{11})CCMSH have proved to be successful in the therapeutic armamentarium of MM due to the fact that they extended the average survival time reducing tumor growth rate and generating remission, moreover, the use of metal-mediated cyclization of the peptides made these molecules resistant to *in vivo* degradation [7–9].

Another point to consider is that alpha-emitting bismuth-213 (^{213}Bi, $T_{1/2}$ =45.6 min, Eα=8.4 MeV) possessing high linear energy transfer (LET) values (≈100 keV/μm) and extremely short α path (40–80 μm) could be widely obtained from Actinum-225/Bismuth-213 (^{225}Ac/^{213}Bi) generator systems [10,11]. State-of-the-art chelating agents for ^{213}Bi radioisotopes such as DOTA and DTPA are well-suited for the creation of strong connection with ^{213}Bi [10]. Taking the above-detailed advantageous characteristics into account, ^{213}Bi-labelled radiopharmaceuticals are considered silver bullet in both diagnostic and therapeutic fields.

Depending upon the LET radiation value, the effect, and the efficacy of MM-specific radioisotopes vary to a great extent. Given the notably high LET value and the short path length of alpha-radiation (2–10 cells), α-emitters exert powerful killing effect on the tumor cells and related microenvironment without imposing significant adverse toxicity on the neighbouring healthy tissues [12]. Based on its high-energy linear transfer, alpha radiation induces enhanced rate of double-strand and cluster DNA breaks as well as base chemical reactions that activate a broad set of intracellular processes associated with apoptotic mechanisms, autophagy, and necrosis [12,13]. Neither the stage of the cell cycle nor the level of oxygenation affects the tumor cell killing effect of the alpha emitters [13,14]. Therefore, these physical properties make them precious candidates in targeted cancer treatment. In contrast, however desired β-emitters may be in the elimination of large tumor masses, the fact that they purvey remarkable radiation and subsequent damage to the non-neoplastic tissues remains a meaningful shortcoming of radiometals with β emission [15]. In addition, Auger electron emitters are characterized by high LET values and ultra-short pathway in human tissues; although their integration into the nucleus of the tumor cells is mandatory to achieve adequate cytotoxic effect [16].

In the present study we aimed at assessing the biodistribution and the melanoma tumor targeting properties of different, newly synthesized MC1-R ligands labelled with ^{213}Bi.

2. Materials and methods

2.1. Chemicals and preparation methods

ABX (Radeberg, Germany) supplied DOTA-NAPamide **(1)**.

Both DOTA-MARSamide (DOTA-Gly-Tyr-Nle-Asp-His-D-Phe-Arg-Trp-Arg-Arg-NH_2) **(2)** and DOTA-FOLDamide (DOTA-Arg-Arg-Gly-Tyr-Nle-Asp-His-D-Phe-Arg-Trp-NH_2) **(3)** were produced by Semmelweis University (Budapest, Hungary). Fig. 1. represents the molecular structure of the different DOTA-conjugated peptides.

DOTA-HOLDamide **(4)** in a form of resin-bound peptide (DOTA$(tBu)_3$-Gly-pY-OBzl-Nle-Asp(OtBu)-His(Trt)-(D-Phe)-Arg(Pbf)-Trp(Boc)-(Rink Amide MBHA resin), 1562 g/mol) was purchased from Caslo (Kongens Lyngby, Denmark). We conditioned the peptide-resin (50.61 mg) by washing it with 10–10 mL of dimethylformamide, acetic acid, dichloromethane, methanol (MeOH) and ether. After that, the resin was dried under vacuum and at atmospheric pressure for one and 24 h; respectively. Following the mixing of the conditioned and dried resin with the solution of trifluoracetic acid (95): triisopropylsilane (2.5): water (2.5)/TFA (95): triisopropylsilane (2.5): water (2.5), the suspension was incubated for 2 h at room temperature. Thereafter, the cleaved resin was filtered out (ISO-DISC PTFE-4 4 mm × 0.45 μm) and washed with 2 mL TFA. An overnight storage of the filtrate occurred at 4 °C. The synthetized, slightly purple solution was evaporated to dryness and re-dissolved in 200 μL TFA. The peptide was then precipitated, filtered out, and washed with 2 mL ether applying a glass filter, and with 1 mL ether, respectively. Finally, it was dried (3.85 mg) and dissolved in 3.85 mL H_2O. DOTA-HOLDamide was identified on a BEH C18 1.7 μm 2.1 × 50 mm column using Waters Acquity I-Class UPLC liquid chromatography system applying PDA detector coupled to a Xevo G2 QT of MS (mass spectrometry).

Raytest miniGita Star TLC (radio-TLC) scanner with plastic scintillator detector was used for the labelling experiments.

The activity of the solution was measured by ISOMED 2010 Dose calibrator at ^{213}Bi and ^{18}F channel.

2.2. Elution of Actinum-225/Bismuth-213 (^{225}Ac/^{213}Bi) Generator

^{225}Ac/^{213}Bi generator (180 MBq) was supplied by the Institute for Transuranium Elements (ITU), Germany. Prior to elution, the column was rinsed with 0.01 M Hydrochloric acid (HCl). Following the elution of ^{213}Bi with the mixture of 600 μL 0.1 M sodium-iodide /0.1 M HCl, the column was repeatedly rinsed and then stored in 0.01 M HCl [11].

2.3. $^{205/206}$ Bi production and purification

The $^{205/206}$Bi isotope mixture was produced in a GE PETtrace cyclotron with 16 MeV proton (60 min, 10 μA) beam on natural Pb-foil target (99.995%, 0.9 by 0.9 cm, 0.25 mm thick). The irradiated Pb target was dissolved in 7 M suprapur HNO_3 (2 mL) and concentrated to circa 1 mL, where $Pb(NO_3)_2$ precipitation was observed. The solution was separated from the solid and diluted to 10 mL with ultrapure (u.p.)

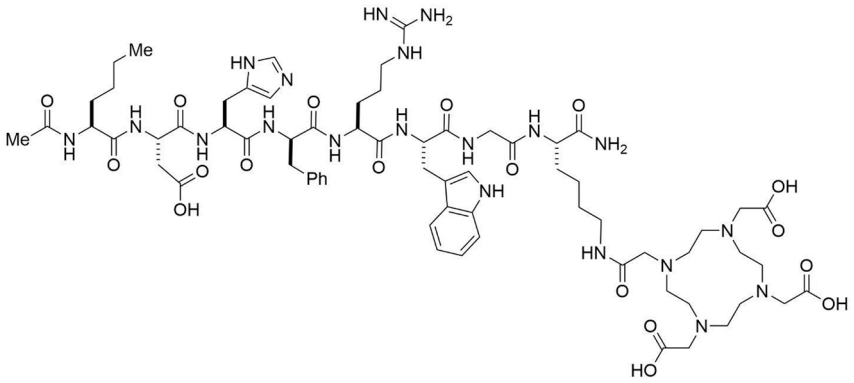

DOTA-NAPamide, 1

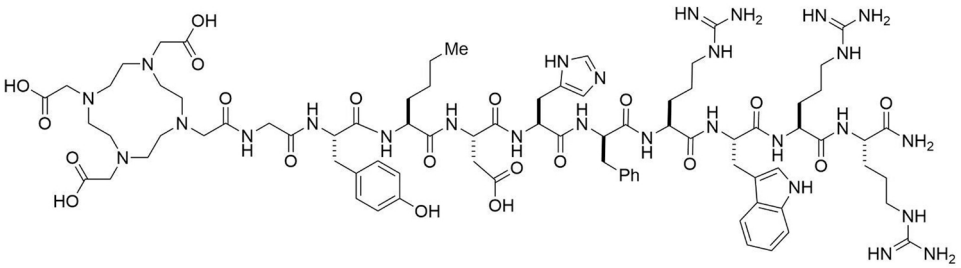

DOTA-MARSamide, 2

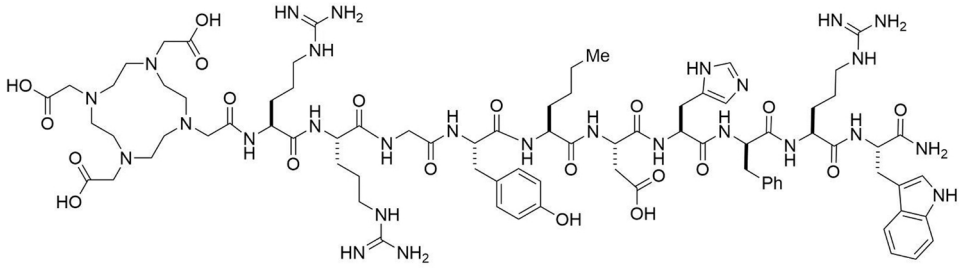

DOTA-FOLDamide, 3

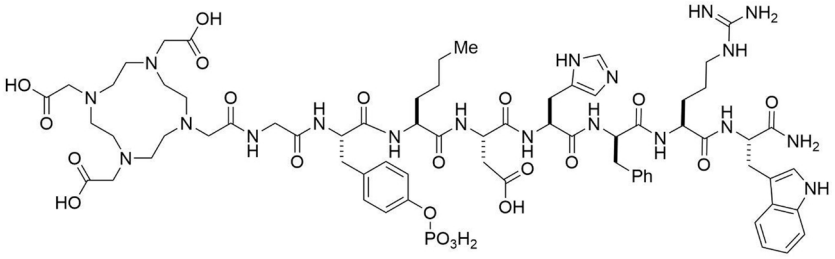

DOTA-HOLDamide, 4

Fig. 1. Molecular structures of the different DOTA-conjugated MC1-R-affine peptides. Fig. 1. presents the molecular structures of the different DOTA-conjugated MC1-R-affine peptides. DOTA: 1,4,7,10-tetraazacyclododecane-1,4,7,10-tetraacetic acid; MC1-R: melanocortin-1 receptor.

water and filtered with Millipore 0.22-μm filter, then transferred onto a column self-filled with 150 mg TK 200 resin (pre-conditioned with 1 mL 0.7 M s.p. HNO_3, 1 mL 7 M s.p. HNO_3 and 5 mL 0.7 M s.p. HNO_3). The column was washed with 5 mL 0.7 M s.p. HNO_3 and the $^{205/206}$Bi isotopes were eluted with 7 M s.p. HNO_3 in 1 mL fractions. The fractions which contained $^{205/206}$Bi isotopes (~30 MBq) were concentrated to dryness and were dissolved in 200 μL 0.1 M u.p. HCl.

2.4. Radiolabelling of DOTA-conjugated peptides

A stock solution of 1 mg/mL was prepared from the DOTA conjugated peptides. In case of the *in vivo* measurements, 5 μL DOTA-NAPamide/DOTA-HOLDamide or 10 μL DOTA-MARSamide and DOTA-FOLDamide solutions corresponding to 3.4, 3.2, 5.6 and 5.6 nmol peptide; respectively were added to 600 μL ^{213}Bi (96.01 ± 17.49 MBq), 135 μL 2 M TRIS buffer (0.34 M) and 50 μL 20% ascorbic acid (72 mM)

at pH 8.7. In case of the determination of the *LogP* values and the stability of the radiolabelled peptides, 20 μL $^{205/206}$Bi was added to the mixture of sodium citrate (pH 5.5, 30–35 μmol) and the stock solution of the DOTA-conjugated peptides (10.1 nmol DOTA-NAPamide, 9.6 nmol DOTA-HOLDamide, 8.4 nmol DOTA-MARSamide and -FOLDamide). The reactions were incubated for 5 min at 95 °C. After cooling to room temperature, the mixture was supplemented with 400 μL 1 M ammonium-acetate (NH_4OAc; pH 4) and was passed through ethanol and water pre-conditioned Solid Phase Extraction (SPE) cartridge (Oasis HLB 1 cc (30 mg) Extraction Cartridge; Waters). The cartridge was then purged with 1 mL water. The dropwise elution of the labelled product from the cartridge into an Eppendorf tube was accomplished utilizing 200 μL ethanol. Thereafter, it was evaporated to dryness at 60 °C in a heating block applying nitrogen stream. The product was dissolved in 200 μL phosphate-buffered saline (PBS) buffer for *in vivo* measurements and in 30 μL PBS for the determination of the *LogP* values and stability. The radiochemical purity was determined on Instant Thin Layer Chromatography impregnated with silica gel (iTLC-SG; Varian) by radio-TLC using 0.1 M sodium citrate (pH 5.5) as mobile phase.

2.5. Determination of LogP values

The octanol/water partition coefficient *(LogP)* is defined as the ratio of a chemical's concentration in the octanol phase to its concentration in the aqueous phase of a two-phase octanol/water system. The following formula was used for the calculation of the *LogP* values:

$$\mathrm{LogP} = \log \frac{[c]octanol}{[c]water}$$

Ten μL of SPE purified labelled peptide in PBS solution was mixed with 0.49 mL water and 0.5 mL 1-octanol in an Eppendorf vial. The mixture was shaken for 30 min applying a vortex shaker (600 rpm). After centrifugation (6000 rpm, 5 min) samples of 100 μL were taken from each phase, and the radioactivity of the fractions was measured with a gamma counter (Perkin Elmer Wizard).

2.6. Determination of the stability of the ^{213}Bi-labelled DOTA-conjugated peptides

Twenty-to-twenty μL of [$^{205/206}$Bi]Bi-DOTA-NAP/HOLD/MARS/FOLDamide solution was added to the solution of 80–80 μL of human plasma. Samples were analyzed by radio-TLC after 5, 30, 60, 90 and 120 min. The analytical conditions were the same as detailed for the quality control of the labelled compound.

2.7. Experimental animals

C57BL/6 J mice (n = 40) kept under conventional laboratory circumstances were enrolled in our present study. The experimental small animals were housed in Individually Ventilated Cages at a temperature of 24 ± 2 °C with 55 ± 10% humidity. Artificial lighting was assured with a circadian cycle of 12 h. Sterile semi-synthetic diet (Akronom Ltd., Budapest, Hungary) as well as drinking water were provided *ad libitum* to all experimental animals. The laboratory animals were obtained and treated in compliance with the criteria of the Ethics Committee for Animal Experimentation of the United Kingdom with the permission of the Ethics Committee for Animal Experimentation of the University of Debrecen (approval number: 16/2022/DEMÁB).

2.8. In vivo melanoma tumor model

Ten-week-old female C57BL/6 J mice (n = 20) were involved in the biodistribution studies. For MC1-R positive melanoma tumor induction, C57BL/6 J mice were subcutaneously *(s.c.)* injected with 1×10^5 MC1-R positive B16-F10 tumor cells in 100 μL saline in the left shoulder area. *Ex vivo* experiments were conducted 14 ± 1 days post-administration of the tumor cells at the tumor volume of 115 ± 10 mm^3.

2.9. Ex vivo biodistribution studies

Ex vivo biodistribution studies were carried out 90 min after the intravenous *(i.v.)* injection of 3.81 ± 0.32 MBq [^{213}Bi]Bi-DOTA conjugated NAPamide, HOLDamide, FOLDamide and MARSamide. Following the euthanization with 5% Forane, tissue samples were taken from both the healthy control and the B16-F10 tumor-bearing experimental animals for weight as well as calibrated gamma counter-based (Packard, Cobra II) radioactivity measurement. The radiopharmaceutical accumulations were then expressed as %ID/g tissue.

2.10. Dose estimation

With the aim of calculating cumulative activities (numbers of disintegrations) in various organs, *ex vivo* biodistribution data were obtained - *as described in the previous section* - from two, three and eight mice 15, - 30, - and 90 min postinjection. The fractional uptake expressed in unit mass (%ID/g) of various organs of different animals was averaged. Two available software packages, OLINDA and IDAC-Dose were used to estimate the equivalent doses of organs and the effective dose.

(a) Based on the method described by Zhou et al. and Kirschner et al. Organ Level Internal Dose Assessment (OLINDA/EXM) version 2.1 (Vanderbilt University) was used to calculate the kinetic values in MBq·h/MBq unit as well as the dose estimates [17,18]. OLINDA utilizes dosimetry data accounting for the full decay scheme of ^{213}Bi, as provided by the Brookhaven National Laboratory data base [19]. Since the average body weight of the experimental animals was 22.2 g, we applied Olinda's smallest mouse model of 25 g [20]. To determine the cumulative activity ratio *(organ residence time x absorbed organ dose)* of the organs separately, at each time point the average of the activity rate per unit organ mass of the corresponding animal was multiplied with the standard mass of the organ. For dose estimation the activity concentrations were multiplied by the organ masses based on the mouse model of 25 g [20]. The ^{213}Bi dose values were extrapolated by OLINDA to the ICRP 89 (Publication 89 of the International Commission on Radiological Protection, [21]) standard human male model, applying multiplication proportional to organ weights [22].

(b) For dose calculations by IDAC-Dose 2.1 [23], first we scaled the fractional organ uptake values using the organ masses in the standard human adult male model of ICRP 110 [24], and then used the kinetic modelling provided by IDAC-Dose to calculate cumulative uptake values for the organs measured (cf. [25]). Then the human equivalent and effective doses were estimated using IDAC-Dose 2.1.

2.11. Statistical analyses

Significance was calculated by two-way ANOVA, Student's t-test (two-tailed) and Mann-Whitney U-test. We set the significance level at $p < 0.05$ unless otherwise indicated. Data are exhibited as mean±SD of at least three independent experiments.

3. Results and discussion

3.1. Characterization of the ^{213}Bi-labelled DOTA-conjugated peptides

Given the limited accessibility of ^{213}Bi, $^{205/206}$Bi^{III} was used as a model isotope for studying the octanol/water partition coefficient and the stability of the $^{205/206}$Bi^{III}-labelled DOTA-conjugated peptides. ^{205}Bi^{III} (100% β^+, $T_{1/2}$ =15.31 d) and ^{206}Bi^{III} (100% β^+, $T_{1/2}$ =6.243 d)

isotopes are produced in cyclotron by the irradiation of natural Pb-foil in approximately 1:2 ratio at 16 MeV proton energy [26]. In shorter experiments - *such as in stability investigations (1 h)* - the decay of the $^{205/206}Bi^{III}$ isotope can be neglected. Octanol/water partition coefficients were calculated for peptides and DOTA-conjugated peptides, while measured for $^{205/206}$Bi-labelled DOTA-conjugated peptides (Fig. 2.). Based on our calculations, the DOTA-HOLDamide was the least hydrophilic, while as for the other peptides hydrophilicity decreased in the following order: DOTA-FOLDamide > DOTA-MARSamide > NAPamide. On the contrary, the octanol/water partition coefficient was found to be -2.25 ± 0.27, -2.33 ± 0.36, -2.43 ± 0.34, and -3.23 ± 0.23, for the [$^{205/206}$Bi]Bi-DOTA HOLDamide, -FOLDamide and -MARSamide; and the NAPamide; respectively. These *LogP* results anticipate that the excretion of the radiotracers occurs via the urinary system. The contradiction between the octanol/water partition coefficient of the DOTA-peptides and the $^{205/206}$Bi-labelled DOTA-peptides may originate from the effect of the metal on the polarity of the tracer. The *LogP* value of [$^{205/206}$Bi]-DOTA-NAPamide was in agreement with the *LogP* values of the [^{68}Ga]Ga-DOTA-NAPamide and [^{44}Sc]Sc-DOTA-NAPamide [3].

The stability of [$^{205/206}$Bi]Bi-DOTA-NAPamide, -HOLDamide, -MARSamide and -FOLDamide were studied in human plasma at 37 °C for 90 min. The stability determination showed that [$^{205/206}$Bi]Bi-DOTA-NAPamide and [$^{205/206}$Bi]Bi-DOTA-HOLDamide suffered ^{213}Bi loss to an extent of 3.5% and 1.4%; respectively. In contrast, no loss of ^{213}Bi was noticed in case of [$^{205/206}$Bi]Bi-DOTA-MARSamide and -FOLDamide. Serum stability measurements indicate that these derivatives remain stable during *in vivo* application (Fig. 3.). MS Spectrometry showed that DOTA-HOLDamide has a peak at 1.80 min retention time on UV chromatogram (254 nm) and 1.99 min on MS TIC chromatogram. ESI$^+$ MS: Exact mass of [$C_{69}H_{96}N_{19}O_{21}P$] = 1557.68 g/mol *m/z*: [M+H$^+$] measured: 1558.78 (expected: 1558.68); [M+ 2 H$^+$] measured: 779.91 (expected: 779.85); [M+ 3 H$^+$] measured: 520.27 (expected:520.23).

The molar activity of [^{213}Bi]Bi-DOTA-NAPamid, -HOLDamide, MARSamide and FOLDamide used *in vivo* were 12.92 ± 4.33 GBq/μmoL, 13.13 ± 2.76 GBq/μmoL, 2.07 and 1.85 GBq/μmoL; respectively.

3.2. Ex vivo biodistribution studies in healthy control and B16-F10 tumor-bearing mice

Ex vivo biodistribution studies were executed 90 min after the *i.v.* injection of the investigated radiotracers into both the healthy control and the B16-F10 tumor-bearing C57BL/6 mice in order to define the normal biodistribution and the tumor targeting potential of [^{213}Bi]Bi-DOTA conjugated NAPamide, HOLDamide, FOLDamide and MARSamide molecules. *Ex vivo* data revealed notable accumulation in the kidneys and in the urine in case of all radiotracers (the detailed values are presented in Table 1.). Rapid renal clearance strengthens the hydrophilic properties of the investigated ^{213}Bi-tagged MC1-R ligands. As part of these experiments, moderate radiotracer accumulation was depicted regarding NAPamide, HOLDamide and MARSamide in the liver (NAPamide, HOLDamide, MARSamide: 1.03 ± 0.23, 0.30 ± 0.05, 1.51 ± 0.17; respectively), the lungs (NAPamide, HOLDamide, MARSamide: 0.25 ± 0.09, 0.13 ± 0.06, 0.71 ± 0.11; respectively), and the spleen (NAPamide, HOLDamide, MARSamide: 0.51 ± 0.26, 0.10 ± 0.03, 0.36 ± 0.08; respectively). In addition, low %ID/g uptake values could be registered in the brain, heart, bone, muscle, the adipose tissue, and in other abdominal organs applying [^{213}Bi]Bi-DOTA conjugated NAPamide, HOLDamide, and MARSamide (as indicated in Table 1.). However, analyzing the *ex vivo* biodistribution data of [^{213}Bi]Bi-DOTA-FOLDamide, significantly ($p < 0.01$) higher radiopharmaceutical accumulation was observed in the majority of the investigated organs and tissues in comparison with that of the three other radiolabelled compounds (seen in Table 1.). The exact reason behind this finding is not yet established, we suppose that it may be partly assigned to the physicochemical properties of [^{213}Bi]Bi-DOTA-FOLDamide and the structure of the peptide. Fast urinary excretion could also be hampered by complexation with plasma proteins. The elevated [^{213}Bi]Bi-DOTA-FOLDamide accumulation registered in the liver (%ID/g:12.86 ± 2.45), in the small intestines (%ID/g:0.68 ± 0.12), in the colon (%ID/g: 1.85 ± 0.25) and in the stomach (%ID/g: 0.72 ± 0.21) may reflect the existence of excretion via the gastrointestinal system. Although the exact mechanism behind enhanced liver uptake remains to be elucidated, the possible role of the hepatic vasculature as well as metabolic factors might also be supposed. Another hypothesis regarding higher hepatic uptake could be related to the mechanism of action of the reticuloendothelial (RES) liver cells. In addition, *ex vivo* measurements disclosed comparatively increased pulmonary accumulation of [^{213}Bi]Bi-DOTA-FOLDamide (%ID/g: 3.11 ± 0.19). According to the explanation of Hajdu et al., prominent lung tracer accretion could be attributed to the prolonged accumulation of this hydrophilic complex in aqueous lung areas [27]. Consequently, the re-entrance of [^{213}Bi]Bi-DOTA-FOLDamide into the circulatory system is extended. We hypothesize that the remarkable lienal tracer uptake (%ID/g: 4.29 ± 1.27) could be caused by RES cell mediated radiopharmaceutical accumulation. Finally, - for all labelled compounds - considerably low (%ID/g: 0.01 ± 0.01)

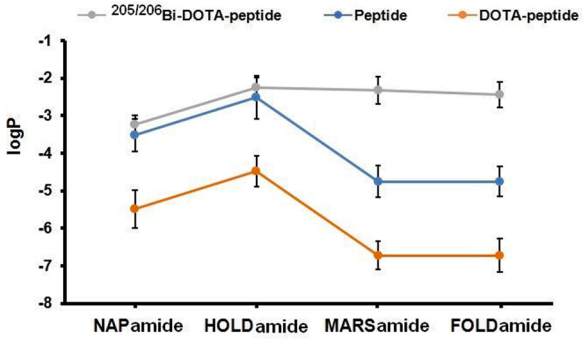

Fig. 2. Partition coefficient of [$^{205/206}$Bi]Bi-DOTA-NAPamide, -HOLDamide, -MARSamide and –FOLDamide. Fig. 2. displays the partition coefficient of [$^{205/206}$Bi]Bi-DOTA-NAPamide, -HOLDamide, -MARSamide and -FOLDamide. Data are expressed as mean±standard deviation (SD). n = 3 measurements/probe. Three independent experiments were performed in triplicate. DOTA: 1,4,7,10-tetraazacyclododecane-1,4,7,10-tetraacetic acid.

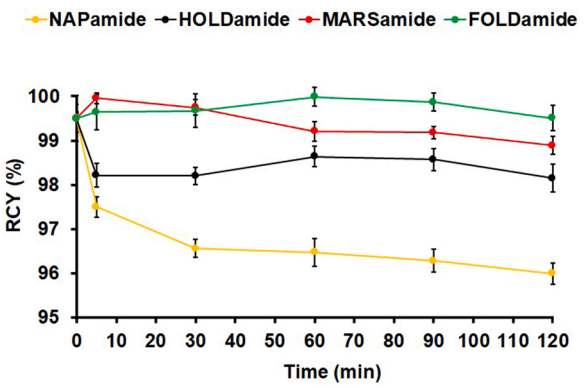

Fig. 3. Results of the plasma stability measurements of the investigated ^{213}Bi-labelled, DOTA-conjugated MC1-R-affine peptides: [^{213}Bi]Bi-DOTA-NAPamide, -HOLDamide, MARSamide and FOLDamide. Fig. 3. presents the results of the plasma stability measurements of the investigated ^{213}Bi-labelled, DOTA-conjugated MC1-R-affine peptides: [^{213}Bi]Bi-DOTA-NAPamide, -HOLDamide, MARSamide and FOLDamide. Data are expressed as mean±standard deviation (SD). n = 3/time point/radiopharmaceutical. Three independent experiments were performed in triplicate. DOTA: 1,4,7,10-tetraazacyclododecane-1,4,7,10-tetraacetic acid; MC1-R: MC1-R: melanocortin-1 receptor; RCY: radiochemical yield.

Table 1
Ex vivo biodistribution data of [^{213}Bi]Bi-labelled DOTA-NAPamide, HOLDamide, MARSamide and FOLDamide in healthy control mice 90 min post-administration of approximately 4 MBq of [^{213}Bi]Bi-DOTA conjugated MC1-R-affine α-MSH-analogue radiopharmaceuticals. %ID/g tissue values are presented as mean±SD. n = 5 animals/radiopharmaceutical. Significance level $p \leq 0.01$ (**). DOTA: 1,4,7,10-tetraazacyclododecane-1,4,7,10-tetraacetic acid; MC1-R: melanocortin-1 receptor; α-MSH: alpha-melanocyte stimulating hormone; SD: standard deviation.

	[^{213}Bi]Bi-DOTA-NAPamide	[^{213}Bi]Bi-DOTA-HOLDamide	[^{213}Bi]Bi-DOTA-MARSamide	[^{213}Bi]Bi-DOTA-FOLDamide
blood	0.17 ± 0.02	0.10 ± 0.03	0.23 ± 0.02	1.41 ± 0.08 * *
urine	27.00 ± 9.90	13.46 ± 2.04	15.23 ± 3.25	12.26 ± 2.07
liver	1.03 ± 0.23	0.30 ± 0.05	1.51 ± 0.17	12.86 ± 2.45 * *
spleen	0.51 ± 0.26	0.10 ± 0.03	0.36 ± 0.08	4.29 ± 1.27 * *
kidney	5.77 ± 1.25	2.85 ± 0.69	6.09 ± 1.21	23.87 ± 4.26 * *
small intestine	0.10 ± 0.01	0.12 ± 0.10	0.15 ± 0.04	0.68 ± 0.12 * *
colon	0.06 ± 0.02	0.08 ± 0.04	0.21 ± 0.05	1.85 ± 0.25 * *
stomach	0.14 ± 0.03	0.10 ± 0.03	0.13 ± 0.03	0.72 ± 0.21 * *
muscle	0.02 ± 0.01	0.01 ± 0.01	0.02 ± 0.01	0.44 ± 0.12 * *
fat	0.02 ± 0.01	0.02 ± 0.02	0.05 ± 0.01	0.09 ± 0.02
lungs	0.25 ± 0.09	0.13 ± 0.06	0.71 ± 0.11	3.11 ± 0.19 * *
heart	0.08 ± 0.01	0.05 ± 0.01	0.14 ± 0.03	0.91 ± 0.12 * *
brain	0.01 ± 0.01	0.01 ± 0.01	0.01 ± 0.01	0.01 ± 0.01
bone	0.03 ± 0.01	0.03 ± 0.03	0.02 ± 0.01	0.03 ± 0.01
salivary glands	0.17 ± 0.08	0.09 ± 0.05	0.10 ± 0.02	0.20 ± 0.08
gall-bladder	0.27 ± 0.01	0.03 ± 0.06	0.12 ± 0.03	0.95 ± 0.17 * *
pancreas	0.07 ± 0.02	0.01 ± 0.02	0.03 ± 0.01	0.40 ± 0.10 * *

cerebral radiotracer uptake was indicated. We presuppose that the blood-brain barrier prevents the entrance of these molecules into the brain.

In the second part of the *ex vivo* biodistribution studies, 14 ± 1 days after tumor transplantation, the MC1-R specificity of [^{213}Bi]Bi-DOTA conjugated NAPamide, HOLDamide, FOLDamide and MARSamide was evaluated in B16-F10 melanoma tumor-bearing small animals 90 min post radiopharmaceutical administration. Based on these *ex vivo* experimental figures, high tumor tracer accumulation was recorded utilizing [^{213}Bi]Bi-DOTA-NAPamide and [^{213}Bi]Bi-DOTA-FOLDamide with uptake values of 3.76 ± 0.96 and 3.28 ± 0.95; respectively. As for [^{213}Bi]Bi-DOTA-HOLDamide considerably lower accumulation (1.93 ± 0.68) was depicted, whereas [^{213}Bi]Bi-DOTA-MARSamide showed the lowest radiopharmaceutical uptake (0.96 ± 0.33; $p < 0.01$). These *ex vivo* biodistribution data are presented in Fig. 4. Analyzing the quantitative figures, [^{213}Bi]Bi-DOTA-NAPamide and [^{213}Bi]Bi-DOTA-FOLDamide would provide images with more contrast in diagnostic settings

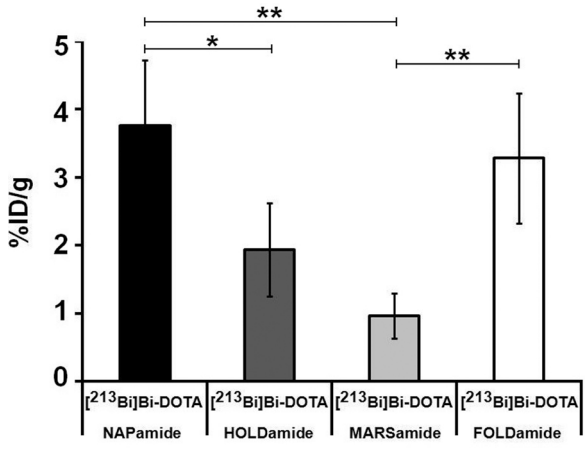

Fig. 4. *Ex vivo* evaluation of [^{213}Bi]Bi-DOTA-NAPamide, -HOLDamide, MARSamide and FOLDamide accumulation in experimental melanoma tumors. Fig. 4. demonstrates the *ex vivo* results of the uptake of [^{213}Bi]Bi-DOTA conjugated NAPamide, HOLDamide, MARSamide and FOLDamide (expressed in % ID/g) in B16-F10 tumors (n = 20) 90 min after the intravenous injection of the radiotracers and 14 ± 1 days post tumor cell inoculation. %ID/g tissue values are presented as mean±SD. n = 5 animals/radiopharmaceuticals. Significance levels: $p \leq 0.05$ (*); $p \leq 0.01$ (**). DOTA: 1,4,7,10-tetraazacyclododecane-1,4,7,10-tetraacetic acid; SD: standard deviation.

compared to the other two derivatives. Given that NAPamide has the best tumor accumulation along with a relatively insignificant hepatic uptake (%ID/g: 1.03 ± 0.23) that leads to enhanced tumor-to-background ratios (T/M), the use of the ^{213}Bi-appended NAPamide probe would ensure high resolution images. According to previous findings, the differences between the tumor uptake of the investigated compounds may stem from the receptor-binding capability, the stability, the chemical as well as the pharmacokinetical properties of the injected radiopharmaceuticals [4]. Although, the exact mechanism behind is not yet covered, future, un-biased studies are warranted to fully address this question. We suppose that the saturation of the receptor-binding sites/reactive sites could possibly explain moderate tumor uptake values.

Analyzing prior research data, researchers disclosed remarkably increased *in vivo* radiolabelled α-MSH analogue uptake in B16-F10 neoplasms in comparison with A375 tumors characterised by low MC1-R expression [3,5]. Tafreshi et al. developed MC1-R receptor expressing MM selective optical probes by producing a fluorescently appended MC1-R-affine peptidomimetic ligand, MC1RL-800 [28]. To assess its *in vivo* tumor specificity, following the *i.v.* injection of nude A375 and A375/MC1R tumorous mice with low and high receptorial expression; respectively, fluorescence imaging was conducted. Based on the significantly increased uptake values of the receptor positive tumors compared to the ones with faint expression ($p < 0.05$), *Tafreshi and colleagues* authenticated the diagnostic value of this labelled MC1-R diagnostic probe [28]. Further, the MC1-R affinity of the radiolabelled NAPamide was already evaluated in former experiments at preclinical level. In one study conducted by *Nagy and colleagues* the MC1-R binding ability of DOTA conjugated NAPamide labelled with ^{44}Sc and ^{68}Ga was confirmed *in vitro* and *in vivo* utilizing MC1-R positive B16-F10 and receptor naïve A375 melanoma cell lines as well as B16-F10 tumorous C57BL/6 J mice and A375 tumor-bearing CB17 severe combined immunodeficient (SCID) mice [3]. Based on the *in vitro* results, - *verifying MC1-R overexpression* - both the ^{68}Ga and ^{44}Sc-appended NAPamide uptake of the B16-F10 cells surpassed that of the A375 cells ($p < 0.01$). As part of their studies, the elevated uptake of [^{44}Sc]Sc-DOTA-NAPamide and [^{68}Ga]Ga-DOTA-NAPamide of the *s.c.* developing receptor positive B16-F10 tumors provided outstanding PET image contrast. However, translational data revealed increased tumor standardized uptake values and T/M ratios in case of the application of the [^{44}Sc]Sc-DOTA-tagged derivative, confirming its superiority in the detection of B16-F10 melanoma cells and tumors. In accordance with their *in vivo* and *ex vivo* outcomes, increased renal accumulation of all investigated derivatives was observed in our study as well. Further, we similarly

depicted either discrete or moderate NAP, - HOLD, - and MARSamide uptake in the abdominal and thoracic organs. In a similar fashion, previous research accomplished with ^{44}Sc and ^{68}Ga-linked DOTA-NAPamide also reported slight radioactivity in the thorax and in almost all of the selected abdominal organs [3]. However, elevated ^{213}Bi-HOLDamide accumulation currently registered in the intestines, in the stomach and in the liver corresponded with results of previous studies dealing with ^{18}F-linked NAPamide derivatives [5].

Although in the present study we did not assess the effects of time or the quantity of peptides on the ex vivo biodistribution pattern of the radiopharmaceuticals, based on current literature data some points are worth mentioning [29,30]. The structure, and the length of the peptides could possibly affect the ex vivo tracer uptake profile of the investigated radiotracers [29]. For example, a shorter peptide counterpart could be associated with more enhanced elimination and wash-out from the non-target organs and tissues. This prompt clearance leads to faint background activity and subsequent improved tumor contrast. Further, shorter molecules might only contain the amino acid motif that is responsible for receptor binding and tumor-targeting since the lack of non-specific peptide segments possibly decreases the development of non-specific binding. In addition, ex vivo measurements performed at several time points would provide additional information regarding the pharmacokinetics of the tracers concerned [30]. Therefore, to better understand the uptake kinetics of the assessed imaging probes, more extended investigations that also focus on the chemical structure of the peptides are warranted.

Based on our results, we observed that the B16-F10 MM neoplasms could be definitively identified with all investigated radiotracers. Given that recent epidemiological data find MM incidence and related death rising, early identification of MC1-R positive tumors is of outstanding clinical significance. The specific tumor accumulation of the evaluated ^{213}Bi-labelled amide derivatives indicates the high affinity of these compounds to MC1-R expressing MM. Therefore, these newly synthesized tumor-targeting radiotracers display excellent potential in the *in vivo* diagnostics of MC1-R positive malignancies that may lead to a breakthrough in the bespoke diagnostic assessment of receptor overexpressing MM. Further, given the alpha emission of these investigated ^{213}Bi-labelled molecules, they could be efficiently exploited in the targeted radionuclid treatment of MC1-R enriched MM. Integration of alpha-emitting, receptor-directed amide derivatives into standard-of-care human protocols could contribute to the establishment of tailor-made MM treatment.

Based on some physical properties of ^{213}Bi; however, its application may pose an issue in both diagnostical and therapeutic medical fields. Besides the necessity of the adjustment of the targeting agent to the short half-life ($T_{1/2}$ =45.6 min) of the radiometal, the therapeutic usage of ^{213}Bi may be restricted when the neoplastic cells are easily reachable for the probe [31]. Given its short-lived nature, further difficulties may arise regarding the transport of the ^{213}Bi-labelled radiopharmaceuticals that could lead to additional financial burden. Another shortcoming that worth mentioning is that the synthesis of ^{213}Bi is not economically viable because of the limited accessibility and the costs of ^{225}Ac [12]. However challenging the integration of ^{213}Bi usage into medicine may be, its superiority over either β-emitters or Auger electrons is undoubtable. As for radionuclides with Auger electron emission, their incorporation into intracellular compartments including the nucleus or the mitochondria or even into the cell membrane is mandatory to obtain radiotherapeutic effects [32]. As remarked above, in case of β-emitters, the undue irradiation of the tumor-naïve healthy tissues represents a significant constraint in clinical settings [15]. Taking into account that the application of ^{213}Bi seems to be a useful means of overcoming the limitations derived from the use of Auger electron and β-emitters, global steps should be taken to combat the drawbacks related to the implementation of α-emitter ^{213}Bi into therapeutic and diagnostic fields.

3.3. Human dose estimation

The fractional cumulative activities (numbers of disintegrations for unit injected activity) of [^{213}Bi]Bi-DOTA-NAPamide in different organs are summarized in Table 2. OLINDA (Vanderbilt University, version 2.1.) and IDAC-Dose 2.1 were used to calculate the equivalent doses of human organs based on the *ex vivo* biodistribution data; the results are presented in Table 3.

Since the two software packages are based on different adult human male models for extrapolating the uptake values and calculating the specific absorbed fractions (OLINDA on ICRP 89 [21] while IDAC-Dose on ICRP 110 [24]), and apply different kinetic models, differences in dose estimates could be expected. With IDAC-Dose, the effective human dose estimate was somewhat lower: $3.63{\cdot}10^{-3}$ mSv/MBq based on ICRP 60 [33] and $4.02{\cdot}10^{-3}$ mSv/MBq based on ICRP 103 [34] vs. $5.52{\cdot}10^{-3}$ mSv/MBq obtained by OLINDA. Similarly, the equivalent doses of the critical organs, the bladder wall ($1.95{\cdot}10^{-2}$ vs. $8.97{\cdot}10^{-2}$) and the kidneys ($7.47{\cdot}10^{-3}$ vs. $5.88{\cdot}10^{-2}$) were considerably lower with IDAC-Dose than with OLINDA.

Although the upscaling of the measurements in mice to human can be considered as rough estimates only, as the discrepancy between the results obtained by the different softwares show, the calculated figures indicate the suitability of the radiolabelled NAPamide derivative as a theranostic agent in the tailor-made treatment of MM.

To our best knowledge no previous research has dealt with the human dose estimation of any types of radiolabelled α-MSH analogues. Neither did we found relevant data in connection with radioactively tagged NAPamide so far. However, given the efficacy of theranostic radiopharmaceuticals, increasing number of studies are centered around the human dose calculation of different theranostics already in clinical use. Pioneering study of Khawar et al. evaluated the distribution of ^{44}Sc-labelled prostate specific membrane antigen-617 ([^{44}Sc]Sc-PSMA-617) and its radiation exposure to normal organs in patients suffering from metastatic castration-resistant prostate cancer [35]. Applying the pharmacokinetics of [^{44}Sc]Sc-PSMA-617 PET/CT imaging they anticipated organ radiation absorbed doses as well as the maximum acceptable radioactivity in patients prior to [^{177}Lu]Lu-PSMA-617 treatment. Due to the renal route of excretion, kidneys with an absorbed dose of 0.319 mSv/MBqm were exposed to the highest radiation danger [35].

4. Conclusion

Currently we were initiated to evaluate the biodistribution and the melanoma targeting potential of the following newly synthesized, ^{213}Bi-labelled DOTA-conjugated MC1-R-affine α-MSH analogues: NAPamide, -

Table 2
Fractional cumulative activities (numbers of disintegrations for unit injected activity) of [^{213}Bi]Bi-DOTA-NAPamide in different organs. DOTA: 1,4,7,10-tetraazacyclododecane-1,4,7,10-tetraacetic acid; LLI: lower large intestines.

	Disintegrations
Organ	**(MBq·h/MBq)**
Brain	$2.50{\cdot}10^{-4}$
LLI contents	$4.25{\cdot}10^{-3}$
Small intestine	$8.87{\cdot}10^{-3}$
Stomach contents	$8.60{\cdot}10^{-4}$
Heart contents	$3.90{\cdot}10^{-3}$
Kidneys	$2.96{\cdot}10^{-2}$
Liver	$2.02{\cdot}10^{-2}$
Lungs	$1.07{\cdot}10^{-3}$
Pancreas	$1.12{\cdot}10^{-3}$
Cortical bone	$7.30{\cdot}10^{-3}$
Spleen	$6.70{\cdot}10^{-4}$
Urinary bladder contents	$1.42{\cdot}10^{-1}$
Total body/remainder	$6.58{\cdot}10^{-2}$
Tumor (0.215 g)	$2.74{\cdot}10^{-3}$

Table 3
Detailed ^{213}Bi equivalent doses (expressed in mSv/MBq) calculated by *IDAC-Dose* after scaling to the ICRP 110 standard adult human male model; and extrapolated by *OLINDA* to the ICRP 89 standard adult human male model. OLINDA: Organ Level Internal Dose Assessment; IDAC: Internal Dose Assessed by Computer; ICRP: International Commission on Radiological Protection.

	Equivalent dose (mGy/MBq)	
Organs	*IDAC*	*OLINDA*
Urinary bladder wall	$1.95 * 10^{-2}$	$8.97 * 10^{-2}$
Kidneys	$7.47 * 10^{-3}$	$5.88 * 10^{-2}$
Osteogenic Cells		$1.01 * 10^{-2}$
Prostate	$2.14 * 10^{-3}$	$1.22 * 10^{-3}$
Stomach wall	$2.04 * 10^{-3}$	$1.12 * 10^{-3}$
Liver	$1.16 * 10^{-3}$	$7.09 * 10^{-3}$
Alveolar-interstitial	$1.15 * 10^{-3}$	
Bronchioles	$1.06 * 10^{-3}$	
Recto-sigmoid colon wall	$1.02 * 10^{-3}$	$1.04 * 10^{-3}$
Small intestine wall	$9.39 * 10^{-4}$	$4.07 * 10^{-3}$
Ureters	$9.16 * 10^{-4}$	
Adrenals	$8.89 * 10^{-4}$	$1.56 * 10^{-3}$
Lung	$8.80 * 10^{-4}$	$6.15 * 10^{-4}$
Right colon wall	$8.71 * 10^{-4}$	$7.10 * 10^{-4}$
Left colon wall	$8.63 * 10^{-4}$	$8.05 * 10^{-3}$
Lymph nodes in sys	$8.61 * 10^{-4}$	
Lymphatic nodes	$7.92 * 10^{-4}$	
Spleen	$7.38 * 10^{-4}$	$2.91 * 10^{-3}$
Pancreas	$5.71 * 10^{-4}$	$5.05 * 10^{-3}$
Muscle	$5.32 * 10^{-4}$	
Lymph nodes (thoracic)	$4.92 * 10^{-4}$	
Skin	$4.62 * 10^{-4}$	
Bronchi bound	$4.28 * 10^{-4}$	
Bronchi sequestered	$4.28 * 10^{-4}$	
Gallbladder wall	$3.68 * 10^{-4}$	$7.86 * 10^{-4}$
ET region	$3.61 * 10^{-4}$	
ET2 basal cells	$3.61 * 10^{-4}$	
Lymph nodes (ET region)	$3.57 * 10^{-4}$	
Testes	$3.19 * 10^{-4}$	$7.24 * 10^{-4}$
Oesophagus	$3.15 * 10^{-4}$	$6.36 * 10^{-4}$
Thyroid	$3.12 * 10^{-4}$	$5.93 * 10^{-4}$
ET1 basal cells	$3.09 * 10^{-4}$	
Heart wall	$2.97 * 10^{-4}$	$3.03 * 10^{-3}$
Red bone marrow	$2.94 * 10^{-4}$	$7.72 * 10^{-4}$
Tonsils	$2.80 * 10^{-4}$	
Pituitary gland	$2.50 * 10^{-4}$	
Breast	$2.45 * 10^{-4}$	
Thymus	$2.13 * 10^{-4}$	$6.14 * 10^{-4}$
Endosteum (bone surface)	$1.86 * 10^{-4}$	
Eye lenses	$1.69 * 10^{-4}$	$5.78 * 10^{-4}$
Salivary glands	$1.51 * 10^{-4}$	$5.84 * 10^{-4}$
Oral mucosa	$1.15 * 10^{-4}$	
Brain	$1.04 * 10^{-4}$	$1.20 * 10^{-4}$
Tongue	$7.73 * 10^{-5}$	
Adipose/residual tissue	$3.78 * 10^{-3}$	
Effective dose (ICRP 60)	$\mathbf{3.63 * 10^{-3}}$	
Effective dose (ICRP 103)	$\mathbf{4.02 * 10^{-3}}$	$\mathbf{5.52 * 10^{-3}}$

HOLDamide, - MARSamide, - and FOLDamide. Given the specific binding capability of the evaluated derivatives to MC1-R overexpressing B16-F10 tumors - *with the highest uptake values of [^{213}Bi]Bi-DOTA-NAPamide and [^{213}Bi]Bi-DOTA-FOLDamide* - these [^{213}Bi]-appended peptide-based molecules could serve as magic bullet for the molecular imaging of MM in the foreseeable future. Finally, besides being valuable diagnostic vectors of receptor positive melanoma, MC1-R-affine analogues labelled with therapeutic radiometals may lead to the establishment of peptide-based bespoke theranostic cancer treatment.

Institutional review board statement

The study was conducted according to the guidelines of the Declaration of Helsinki and approved by the Institutional Animal Care Committee of the University of Debrecen, Hungary (permission number: 16/2022/DEMÁB), and conducted in accordance with the local guidelines and provisions for the implementation of the Animal Welfare Act as well as the regulations of the Federation of Laboratory Animal Science Associations (FELASA).

Informed consent statement

Not applicable.

Conflicts of Interest

The authors declare no conflict of interest.

Funding

The research was supported by the KDP-2021 program of the Ministry for Innovation and Technology from the source of the national research, development and innovation fund (Gy.T. and I. K-SZ.) The published work was supported by the Thematic Excellence Programme (TKP2020-NKA-04) of the Ministry for Innovation and Technology in Hungary. We are grateful to the Hungarian Research Foundation (OTKA ANN 139484). The financial support of the National Research, Development and Innovation Office (TKP2021-EGA-31) is acknowledged. Project no. RRF-2.3.1–21-2022-00015 has been implemented with the support provided by the European Union.

CRediT authorship contribution statement

György Trencsényi: Conceptualization, Visualization, Writing – original draft, Writing – review & editing; **Ildikó Garai:** Conceptualization, Visualization; **József Varga:** Data curation, Methodology, Visualization, Writing – review & editing; **Dezső Szikra:** Conceptualization, Validation; **Dániel Szücs:** Investigation; **Anikó Fekete:** Validation; **Adrienn Vágner:** Investigation, Writing original draft; **István Mándity:** Conceptualization, Methodology; **Zita Képes:** Writing original draft; **Gábor Nagy:** Investigation, Writing – original draft; **Barbara Gyuricza:** Investigation; **János Elek:** Methodology, Writing – review & editing; **Levente Kárpáti:** Conceptualization, Methodology; **Viktória Arató:** Investigation; **Ibolya Kálmán-Szabó**: Investigation; **Frank Bruchertseifer:** Writing – review & editing.

Declaration of Competing Interest

The authors declare that they have no known competing financial interests or personal relationships that could have appeared to influence the work reported in this paper.

Data Availability

The datasets used and/or analysed during the current study are available from the corresponding author upon reasonable request.

References

[1] M.G. Davey, N. Miller, N.M. McInerney, A review of epidemiology and cancer biology of malignant melanoma, Cureus 13 (2021), e15087.
[2] H. Shi, Z. Cheng, MC1R and melanin-based molecular probes for theranostic of melanoma and beyond, Acta Pharmacol. Sin. 43 (2022) 3034–3044.
[3] G. Nagy, N. Dénes, A. Kis, J.P. Szabó, E. Berényi, I. Garai, P. Bai, I. Hajdu, D. Szikra, G. Trencsényi, Preclinical evaluation of melanocortin-1 receptor (MC1-R) specific 68Ga- and 44Sc-labeled DOTA-NAPamide in melanoma imaging, Eur. J. Pharm. Sci. 106 (2017) 336–344.
[4] Z. Cheng, J. Chen, Y. Miao, N.K. Owen, T.P. Quinn, S.S. Jurisson, Modification of the structure of a metallopeptide: synthesis and biological evaluation of 111In-labeled DOTA-conjugated rhenium-cyclized alpha-MSH analogues, J. Med. Chem. 45 (2002) 3048–3056.
[5] Z. Cheng, L. Zhang, E. Graves, Z. Xiong, M. Dandekar, X. Chen, S.S. Gambhir, Small-animal PET of melanocortin 1 receptor expression using a 18F-labeled alpha-melanocyte-stimulating hormone analog, J. Nucl. Med 48 (2007) 987–994.
[6] Y. Miao, K. Benwell, T.P. Quinn, 99mTc- and 111In-labeled alpha-melanocyte-stimulating hormone peptides as imaging probes for primary and pulmonary metastatic melanoma detection, J. Nucl. Med 48 (2007) 73–80.

[7] Y. Miao, N.K. Owen, D.R. Fisher, T.J. Hoffman, T.P. Quinn, Therapeutic efficacy of a 188Re-labeled alpha-melanocyte-stimulating hormone peptide analog in murine and human melanoma-bearing mouse models, J. Nucl. Med 46 (2005) 121–129.
[8] Y. Miao, M. Hylarides, D.R. Fisher, T. Shelton, H. Moore, D.W. Wester, A. R. Fritzberg, C.T. Winkelmann, T. Hoffman, T.P. Quinn, Melanoma therapy via peptide-targeted {alpha}-radiation, Clin. Cancer Res 11 (2005) 5616–5621.
[9] Y. Miao, T.J. Hoffman, T.P. Quinn, Tumor-targeting properties of 90Y- and 177Lu-labeled alpha-melanocyte stimulating hormone peptide analogues in a murine melanoma model, Nucl. Med. Biol. 32 (2005) 485–493.
[10] S. Ahenkorah, I. Cassells, C.M. Deroose, T. Cardinaels, A.R. Burgoyne, G. Bormans, M. Ooms, F. Cleeren, Bismuth-213 for Targeted Radionuclide Therapy: From Atom to Bedside, Pharmaceutics 13 (2021) 599.
[11] A. Morgenstern, F. Bruchertseifer, C. Apostolidis, Bismuth-213 and actinium-225 – generator performance and evolving therapeutic applications of two generator-derived alpha-emitting radioisotopes, Curr. Radiopharm. 5 (2012) 221–227.
[12] Y. Dekempeneer, M. Keyaerts, A. Krasniqi, J. Puttemans, S. Muyldermans, T. Lahoutte, M. D'huyvetter, N. Devoogdt, Targeted alpha therapy using short-lived alpha-particles and the promise of nanobodies as targeting vehicle, Expert. Opin. Biol. Ther. 16 (2016) 1035–1047.
[13] F. Lacoeuille, N. Arlicot, A. Faivre-Chauvet, Targeted alpha and beta radiotherapy: an overview of radiopharmaceutical and clinical aspects, Med. Nucl. 42 (2018) 32–44.
[14] J.P. Pouget, I. Navarro-Teulon, M. Bardiès, N. Chouin, G. Cartron, A. Pèlegrin, D. Azria, Clinical radioimmunotherapy–the role of radiobiology, Nat. Rev. Clin. Oncol. 8 (2011) 720–734.
[15] L. Marcu, E. Bezak, B.J. Allen, Global comparison of targeted alpha vs. targeted beta therapy for cancer: In vitro, in vivo and clinical trials, Crit. Rev. Oncol. Hematol. 123 (2018) 7–20.
[16] H. Fourie, S. Nair, X. Miles, D. Rossouw, P. Beukes, R.T. Newman, J.R. Zeevaart, C. Vandevoorde, J. Slabbert, Estimating the relative biological effectiveness of auger electron emitter 123I in human lymphocytes, Front. Phys. 8 (2020), 567732.
[17] X. Zhou, P.H. Elsinga, S. Khanapur, R.A.J.O. Dierckx, E.F.J. de Vries, J.R. de Jong, Radiation dosimetry of a novel adenosine A2A receptor radioligand [11C] preladenant based on PET/CT imaging and ex vivo biodistribution in rats, Mol. Imaging Biol. 19 (2017) 289–297.
[18] A.S. Kirschner, R.D. Ice, W.H. Beierwaltes, Radiation dosimetry of 131I-19 Iodocholesterol: the pitfalls of using tissue concentration data-reply, J. Nucl. Med 16 (1975) 248–249.
[19] M.G. Stabin, L.C. da Luz, Decay data for internal and external dose assessment, Health Phys. 83 (2002) 471–475.
[20] M.A. Keenan, M.G. Stabin, W.P. Segars, M.J. Fernald, RADAR realistic animal model series for dose assessment, J. Nucl. Med 51 (2010) 471–476.
[21] I.C.R.P. Basic, Anatomical and physiological data for use in radiological protection: reference values. a report of age- and gender-related differences in the anatomical and physiological characteristics of reference individuals, ICRP publication 89, Ann. Icrp. 32 (2002) 5–265.
[22] F. Cicone, T. Denoël, S. Gnesin, N. Riggi, M. Irving, G. Jakka, N. Schaefer, D. Viertl, G. Coukos, J.O. Prior, Preclinical evaluation and dosimetry of [111In]CHX-DTPA-scFv78-Fc targeting endosialin/tumor endothelial marker 1 (TEM1), Mol. Imaging Biol. 22 (2020) 979–991.
[23] M. Andersson, L. Johansson, K. Eckerman, S. Mattsson, IDAC-Dose 2.1, an internal dosimetry program for diagnostic nuclear medicine based on the ICRP adult reference voxel phantoms, EJNMMI Res 7 (2017) 88.
[24] I.C.R.P. Adult, Reference computational phantoms, ICRP Publ. 110. Ann. ICRP 39 (2009) 1–164.
[25] N. Ukon, S. Zhao, K. Washiyama, N. Oriuchi, C. Tan, S. Shimoyama, M. Aoki, H. Kubo, K. Takahashi, H. Ito, Human dosimetry of free ^{211}At and meta-[^{211}At] astatobenzylguanidine (^{211}At-MABG) estimated using preclinical biodistribution from normal mice, EJNMMI Phys. 7 (2020) 1–14.
[26] R. Fischer, J. Wendel, B. Dresow, V. Bechtold, H.C. Heinrich, 205Bi/206Bi cyclotron production from Pb-isotopes for absorption studies in humans, Appl. Radiat. Isot. 44 (1993) 1467–1472.
[27] I. Hajdu, J. Angyal, D. Szikra, I. Kertész, M. Malanga, É. Fenyvesi, L. Szente, M. Vecsernyés, I. Bácskay, J. Váradi, P. Fehér, Z. Ujhelyi, G. Vasvári, Á. Rusznyák, G. Trencsényi, F. Fenyvesi, Radiochemical synthesis and preclinical evaluation of 68Ga-labeled NODAGA-hydroxypropyl-beta-cyclodextrin (68Ga-NODAGA-HPBCD), Eur. J. Pharm. Sci. 128 (2019) 202–208.
[28] N.K. Tafreshi, X. Huang, V.E. Moberg, N.M. Barkey, V.K. Sondak, H. Tian, D. L. Morse, J. Vagner, Synthesis and characterization of a melanoma-targeted fluorescence imaging probe by conjugation of a melanocortin 1 receptor (MC1R) specific ligand, Bioconjug. Chem. 23 (2012) 2451–2459.
[29] J. Chen, M.F. Giblin, N. Wang, S.S. Jurisson, T.P. Quinn, In vivo evaluation of 99mTc/188Re-labeled linear alpha-melanocyte stimulating hormone analogs for specific melanoma targeting, Nucl. Med. Biol. 26 (1999) 687–693.
[30] Y. Miao, N.K. Owen, D. Whitener, F. Gallazzi, T.J. Hoffman, T.P. Quinn, In vivo evaluation of 188Re-labeled alpha-melanocyte stimulating hormone peptide analogs for melanoma therapy, Int. J. Cancer 101 (2002) 480–487.
[31] A. Majkowska-Pilip, W. Gawęda, K. Żelechowska-Matysiak, K. Wawrowicz, A. Bilewicz, Nanoparticles in targeted alpha therapy, Nanomater. (Basel) 10 (2020) 1366.
[32] A.A. Rosenkranz, T.A. Slastnikova, G.P. Georgiev, M.R. Zalutsky, A.S. Sobolev, Delivery systems exploiting natural cell transport processes of macromolecules for intracellular targeting of Auger electron emitters, Nucl. Med. Biol. 80- 81 (2020) 45–56.
[33] ICRP, Recommendations of the international commission on radiological protection, ICRP Publication 60, Ann. Icrp. 21 (1991) (1990) 1–201.
[34] ICRP, The 2007 recommendations of the international commission on radiological protection, ICRP Publication 103, Ann. Icrp. 37 (2007) 1–332.
[35] A. Khawar, E. Eppard, J.P. Sinnes, F. Roesch, H. Ahmadzadehfar, S. Kürpig, M. Meisenheimer, F.C. Gaertner, M. Essler, R.A. Bundschuh, [44Sc]Sc-PSMA-617 biodistribution and dosimetry in patients with metastatic castration-resistant prostate carcinoma, Clin. Nucl. Med. 43 (2018) 323–330.